SSRG International Journal of Electrical and Electronics Engineering
ISSN: 2348-8379/ https://doi.org/10.14445/23488379/IJEEE-V11I4P102

Volume 11 Issue 4, 8-13, April 2024

Original Article

Study of Humanoid Robot's E-Skin with Piezoresistive Nanocomposite Based Tactile Sensors Modelling

Riyaz Ali Shaik[1], Elizabeth Rufus[2]

[1,2]*School of Electronics Engineering, VIT University, Tamil Nadu, India.*

[2]*Corresponding Author : elizabethrufus@vit.ac.in*

Received: 03 February 2024 Revised: 03 March 2024 Accepted: 01 April 2024 Published: 30 April 2024

Abstract *- Piezoresistive nanocomposites are often used as the active layer in the tactile sensors of Electronic Skin (E-skin) for humanoid robots, mostly for static measurements. This study describes the modelling and simulation of three distinct piezoresistive polymer composite materials: Conductive PDMS (CPDMS, a combination of carbon black and PDMS), Polydimethylsiloxane with Multi-Wall Carbon Nano Tubes (PDMS + MWCNT), and MWCNT + Styrene-Butadiene-Styrene (MWCNT + SBS). A generic template of a pressure sensor is modelled on a polyimide substrate and the aforementioned composite materials with optimum weight (wt.) ratios of the CNT as the sensory layer. The mechanical and electrical characteristics of these flexible pressure sensors are simulated, considering real-time environmental conditions. In our study, modelling of the PDMS+MWCNT active layer resulted in a linear response over a wide range of upto 12N of applied tension, while MWCNT + SBS (4% wt.), with a Young's Modulus(E) of 60.4MPa resulted the most conformable sensor, with a maximum displacement of 8.601 x 1013 for 100Pa load. Additional physical aspects that are simulated include the influence of substrate thickness on sensor sensitivity, as well as the validation of the sensor response by putting the active material on both the surface and subsurface layers of an Ecoflex substrate. The resistance changes of the MWCNT + PDMS nanocomposite were simulated and compared to a real-time sensor with a similar physical design, demonstrating consistency between the two. The simulated research of the physical and electrical characteristics yielded a comprehensive comprehension of the sensor's behavior prior to the fabrication of an actual sensor in real time.*

Keywords *- Flexible tactile sensor, Humanoid robot's E-skin, Piezoresistive polymer nanocomposites, Screen-printing, Pressure sensor modelling.*

1. Introduction

Skin is the largest sensory organ in the whole human body, including many proprioceptive cells. Similarly, humanoid robots are enveloped with E-skin that has many sorts of touch sensors. These tactile sensors may use many principles of transduction, such as capacitive [1], optical [2], piezoelectric [3], resistive [4], piezoresistive [5], etc.

However, any tactile sensors based on Electronic skin (E-skin) must possess high conformability, durability, and reliability to serve the purpose of E-skin. Furthermore, bionic artificial skins are developed which not only substitute functionality of permanently damaged tissues but also facilitate self-healing of the wounds. Hence, touch sensors integrated into the E-skin must meet the necessary physical and electrical requirements for proper operation.

The E-skin has a crucial role in measuring static tactile data, and the most suited transduction mechanism for this purpose is piezoresistive. Contemporary printed electronics use piezoresistive sensors that consist of a nanocomposite active layer. This layer is created using an elastomer to provide mechanical flexibility and Carbon Nanotubes (CNT) to enable electrical conduction when static normal pressure is applied.

Preparing the nanocomposite paste is a difficult operation since certain weight ratios of the Carbon Nanotubes (CNT) must be added to the elastomer to get the desired viscosity for screen printing. Additionally, if the paste is created but not utilized, it has the potential to become carcinogenic over time. [6] The excessive filling of Multi-Walled Carbon Nanotubes (MWCNT) agglomerates leads to the formation of a rigid paste that is not suited for the process of printing.

Conversely, a smaller fraction leads to less electrical conductivity and decreased viscosity of the paste. Hence, this research presents a simulation study that investigates the mechanical and electrical characteristics of the sensor at various weight ratios of the active layer using three distinct piezoresistive polymer materials. The discussion in section 2 focuses on the material characteristics of the piezoresistive nanocomposite material employed in the simulation. The discussion in section 3 focuses on the simulation software's working environment and the settings used to reproduce real-time sensors accurately. Section 4 examines the simulation findings to assess the sensor's physical and electrical simulation response.

2. Material Properties of Piezoresistive Polymers

Pressure sensing applications in printed electronics use either capacitive or piezoresistive transduction for tactile sensors. Piezoresistive tactile sensors may be effectively enclosed to minimize crosstalk when arranged in a grid matrix configuration, in contrast to capacitive sensors.

Furthermore, tactile sensors that are based on piezoresistive technology provide exceptional sensitivity and consistency when measuring static quantities [7]. These devices can be produced inexpensively and have a simple interface, making them well-suited for use in large-scale printed electronics, such as the electronic skin of humanoid robots. Piezoresistive active layers are vulnerable to fluctuations in temperature.

The piezoresistive materials examined in this work are PDMS + MWCNT, CPDMS, and MWCNT + SBS. When Multi-Walled Carbon Nanotubes (MWCNT) are mixed with a silicone elastomer, the resulting material is called PDMS + MWCNT. On the other hand, when MWCNT is mixed with a thermoplastic elastic co-polymer like SBS, the resulting material is called MWCNT + SBS. CPDMS does not distribute Carbon Nanotubes (CNTs) inside it; rather, the carbon present in CPDMS amplifies its electrical reaction.

The characteristics of the Multi-Walled Carbon Nanotubes (MWCNT) used in the simulation are as follows: The piezoresistive nanocomposites discussed here have distinct applications. PDMS + MWCNT is commonly used as a pressure sensor that relies on touch [8].

CPDMS is the preferred choice for a micro fingerprint sensor [9]. SBS + MWCNT is used when dealing with significant strains [10]. Pressure sensing applications in printed electronics use either capacitive or piezoresistive transduction for tactile sensors. Piezoresistive tactile sensors may be effectively enclosed to minimize crosstalk when arranged in a grid matrix configuration, in contrast to capacitive sensors.

Furthermore, tactile sensors that are based on piezoresistive technology provide exceptional sensitivity and consistency when measuring static quantities [7]. These devices can be produced inexpensively and have a simple interface, making them well-suited for use in large-scale printed electronics, such as the electronic skin of humanoid robots. Piezoresistive active layers are vulnerable to fluctuations in temperature.

2.1. Printability and Conductivity

Screen-printed touch sensors significantly decrease the manufacturing cost. Therefore, it is necessary to develop a piezoresistive sensor material paste that is suited for screen printing applications. A reduced concentration of Carbon Nanotubes (CNTs) in the material paste hinders electrical conduction, whereas a higher concentration of CNTs leads to increased viscosity of the paste.

Therefore, it is necessary to determine a verified weight ratio to produce a sensor active layer that has both excellent conductivity and the ability to be printed. The literature research conducted in this study indicates that the three piezoresistive materials, namely MWCNT + SBS, PDMS + MWCNT, and CPDMS, meet our specified criteria at weight percentages of 4%, 18% and 20%, correspondingly [11-13]. All simulations conducted in this work only include attributes of active layers with the aforementioned weight ratios.

3. Modelling Geometry and Simulation Parameters

3.1. Physical Modelling

In this study, a generic template has been created using COMSOL Multiphysics 5.3v simulation software. The purpose of this template is to analyze the mechanical and electrical behavior of all three piezoresistive sensors (see Figure 1). The program employs a sequential methodology for sensor design and modelling, akin to the process of real-time screen printing. The integrated database has a diverse selection of polymers, semiconductors, metals, and other materials that may be used.

The generic template is modelled with a polyimide material as its substrate with dimensions of 100 x 100 x 0.5 mm3. A single node sensor block with an area of 10mm x 10mm x 4mm is positioned at the center above the substrate. The sensor node experiences a normal force from a polyimide load block measuring 5mm x 5mm x 4mm, which is positioned underneath the substrate. The substrate and load block are defined with polyimide material elastic properties, whereas the sensor block has material properties specific to the piezoresistive active layer of our interest.

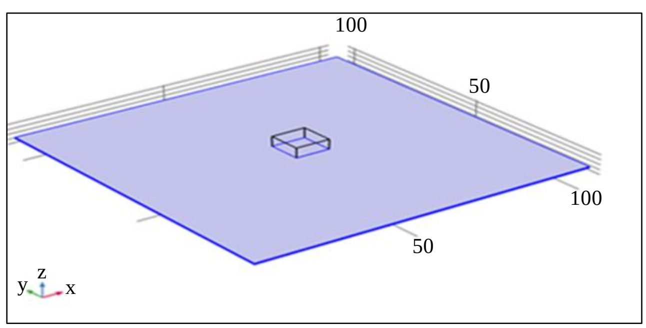

Fig. 1 Generic template of the pressure sensor with polyimide substrate and sensory layer block at the center (Not shown: Load block beneath the substrate and sensory layer)

To measure the piezoresistive response, it is imperative to explore the stress-strain relationship derived from the generalized Hooke's law as the elasticity matrix and also the piezo-coefficient matrix of the material. The elasticity matrix of anisotropic materials is defined using their engineering constants, as shown in Equation 1.

$$\begin{bmatrix}\varepsilon_{11}\\ \varepsilon_{22}\\ \varepsilon_{33}\\ \varepsilon_{23}\\ \varepsilon_{12}\\ \varepsilon_{13}\end{bmatrix} = \begin{bmatrix} 1/E & -v/E & -v/E & 0 & 0 & 0\\ -v/E & 1/E & -v/E & 0 & 0 & 0\\ -v/E & -v/E & 1/E & 0 & 0 & 0\\ 0 & 0 & 0 & 1/\mu & 0 & 0\\ 0 & 0 & 0 & 0 & 1/\mu & 0\\ 0 & 0 & 0 & 0 & 0 & 1/\mu \end{bmatrix} \begin{bmatrix}\sigma_{11}\\ \sigma_{22}\\ \sigma_{33}\\ \sigma_{23}\\ \sigma_{12}\\ \sigma_{13}\end{bmatrix} \quad (1)$$

The engineering constants, namely Shear modulus (μ), Poisson ratio (v), and Young's Modulus (E), exhibit variations based on the material used and their values fed are shown in Table 1. In this study, no shear modulus ($\mu = 0$) is applied.

Table 1. Hooke's law-based elasticity matrix parameters for modelling

Material Used	Poisson Ratio(ν)	Young's Modulus (E)
PDMS+ MWCNT	5.7	4.491 Mpa
CPDMS	3.2	2.452 Mpa
SBS + MWCNT	3	60.43 Mpa
Polyimide	0.32	$3.13e^3$ Mpa

In terms of simulation, the substrate edge limits are immovable, and the static pressure is applied to the sensor from the load block's negative z-direction. The program uses the parametric sweep option to assess the sensor's performance across various pressure values and substrate thickness levels. This parametric sweep yields multiple results considering different parametric values in a single execution.

3.2. Computation of Total Resistance of Nanocomposite Sensory Layer MWCNT +PDMS (18% wt.)

The total resistance of a nanocomposite can be computed from Equation 2.

$$R_{tot}(\varepsilon) = R_s + \frac{1}{|t^2|}\frac{h}{8e^2}\{1 + \exp[\frac{E_g}{KT}]\} \quad (2)$$

By substituting the general SI units for h(Planck's Constant), e(Electron Charge), T(Absolute temperature), K(Boltzmann's Constant) and considering the contact resistance (Rs = 13KΩ) for gold electrode [14] in (2), it is simplified to Equation 3.

$$R_{tot} = 13k + 0.05\ (108)\ [E_g] \quad (3)$$

To compute the CNT energy band gap (Eg) of the material in Equation 3, the physical properties of the CNTs are considered along with zero energy bandgap (E_g^0).

$$E_g^0 = \frac{|p|2\gamma a_0}{\sqrt{3}d} \quad (4)$$

The physical properties of the CNT are taken from the datasheet of the material [15] as chiral angle (θ) = 30°, Hopping Integral (γ) = 2.6eV, diameter of 20nm (d), lattice unit vector length of graphene is ~ 2.49 A° (a_0) and p = +1 represents the positive semiconductor family of the CNT. Substituting these values in Equation 4 results in;

$$E_g^0 = 0.65eV \quad (5)$$

Further energy band gap, zero energy band and volumetric strain (ε) are related as Equation 6.

$$E_g = E_g^0 + \frac{dE_g}{d\varepsilon}\varepsilon \quad (6)$$

The value of the ratio '*dEg/d*ε' of a CNT material is given by Equation 7.

$$\frac{dE_g}{d\varepsilon}\varepsilon = sign(2p+1)3\gamma[(1+v)\cos 3\theta_t] \quad (7)$$

The computed values from Equation 5 and Equation 7, substituted in Equation 6, result in Equation 8.

$$E_g = 0.65eV + (43.51eV)\ \varepsilon \quad (8)$$

The volumetric strain (ε) from the simulation is substituted in Equation 8, and finally, the total change of resistance is deduced using Equation 2 as;

$$R_{tot} = 13k + 0.05(10^8)(0.65eV + (43.51eV)\ \varepsilon) \quad (9)$$

Equation 9 computes the total resistance of the nanocomposite material after obtaining simulated volumetric strain values of the material from the generic template model.

4. Results and Discussion

Simulated mechanical aspects of the tactile sensor are;

4.1. Total Displacement of the Sensor

The load block applies a pressure within the range of 0 to 100KPa onto the sensor. The tactile sensor with the greatest Young's modulus is anticipated to exhibit the largest overall displacement. The total displacement of the pressure sensor with 3 different nanocomposite active layers is shown in Table 2. Figure 2 displays the displacement plot of the sensor, consisting of MWCNT + SBS, in relation to the substrate. MWCNT + SBS nanocomposite has a Young's modulus of 60.4 MPa, which is the highest among the three materials. As a result, it has also generated the most overall displacement.

Table 2. Total displacement simulation response

Sensory Layer	Total Displacement
CPDMS	7.452×10^{13}
SBS + MWCNT	8.613×10^{13}
PDMS+ MWCNT	5.131×10^{13}

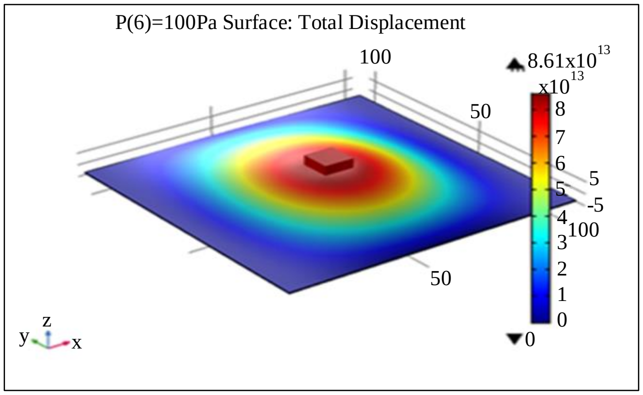

Fig. 2 Total displacement of the pressure sensor with sensory layer as MWCNT+SBS material

4.2. Variation of Substrate Thickness

In a separate mechanical aspect simulation, the thickness of the substrate is altered starting at 1mm and increasing by 0.5mm until it reaches 5mm. According to the literature, [16] the sensitivity of the E-skin decreases as the thickness of the substrate grows. The simulation findings shown in Figure 3 indicated that there is a 50% decrease in the output of the touch sensor for every 0.1 cm increase in substrate thickness.

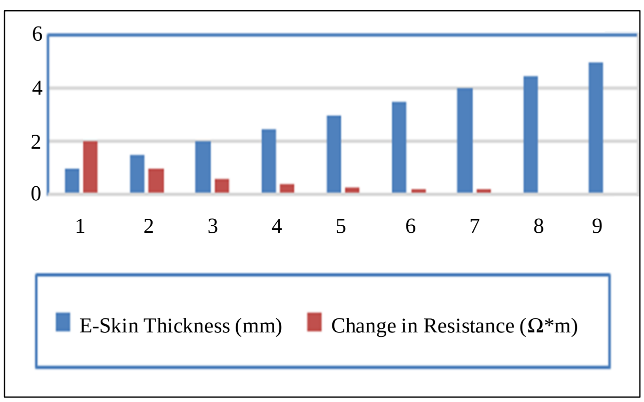

Fig. 3 Response of change in resistance of sensory layer with variation in substrate thickness

4.3. Superficial Layer and Subsurface Layer Geometry

Industrial and commercial humanoid robots need the execution of tasks in a repeated manner. The robot's E-skin must be able to withstand elongation fractures, endure wear and tear, and address adhesion problems in the active layer. In order to tackle these issues, a commercially accessible Ecoflex material is used as a substrate, possessing an elongation break occurring at a strain range of 800% to 1000%. [17] Ecoflex is extensively used as a soft material with a long life in the animatronics sector and the making of children's toys, where repeated and substantial deformations are expected.

[18] This simulation demonstrates the reaction of the tactile sensors when positioned over the substrate surface (superficial) and engrossed into the substrate (sub-surface). The design has an Ecoflex substrate of 10mm x 5mm x 1mm, together with a piezoresistive sensor strip made of MWCNT + PDMS (18% wt.). The sensor strip has dimensions of 5mm x 1mm x 0.1mm. Both subsurface and superficial versions, seen in Figures 4(a) and 4(b) correspondingly, use this geometry.

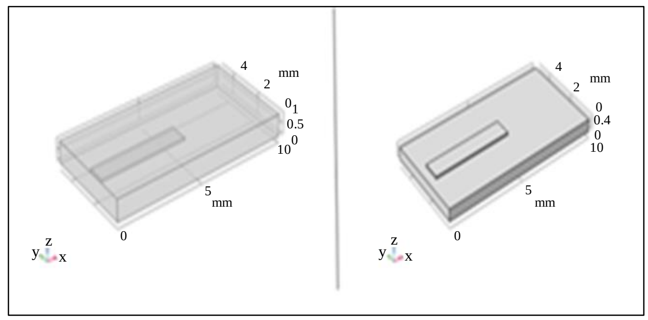

(a) **(b)**

Fig. 4 (a) Geometric design of engrossed subsurface leyer (left), and (b) Geometric design of superficial layer on the substrate.

In the case of subsurface geometry, the active layer is etched at a depth of 0.5mm from the Ecoflex substrate top surface. The Ecoflex material's elastic parameters are reported to have a Young's modulus of 125 KPa and a Poisson ratio of 0.42. [16] The characteristics of the active layer have been previously stated in section 3.1. The stress analysis of both sub-surface and superficial geometries is shown below in Figures 5 and 6, respectively.

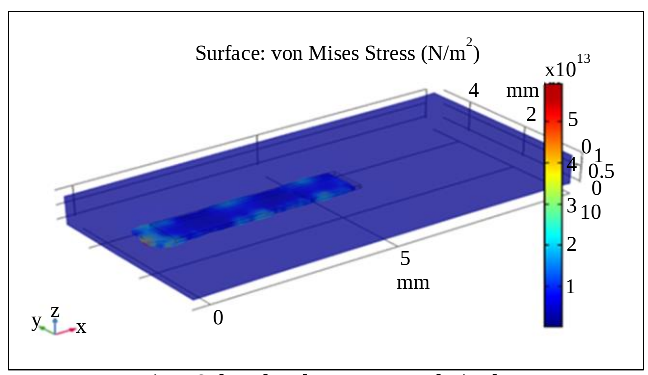

Fig. 5 Subsurface layer stree analysis plot

The superficial model demonstrates greater output consistency at high stresses in comparison to the subsurface model, as anticipated. The superficial model has a higher surface stress of 3.5 x 104 N/m2, in contrast to the subsurface geometry, which has a surface stress of 5 x 103 N/m2. This clearly suggests that the superficial layers are more sensitive and capable of withstanding greater stresses compared to the subsurface layers. Another ongoing problem associated with subsurface geometry is the need for a specialized production procedure, which might potentially compromise the mechanical integrity of the tactile sensor.

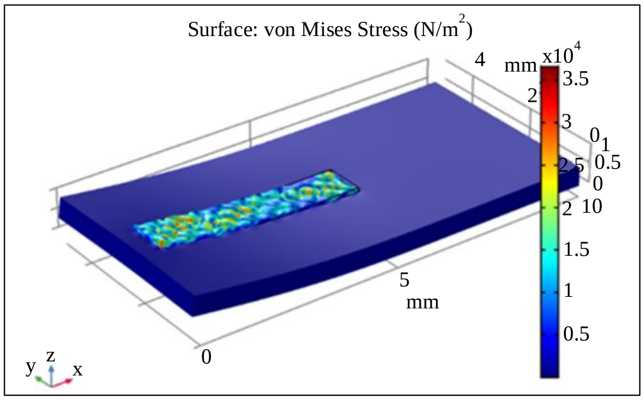

Fig. 6 Superficial layer stress analysis plot

4.4. Validation of Simulated Piezoresistive Response with Real-Time Model

A real-time tactile sensor, using a screen-printed active layer composed of PDMS (polydimethylsiloxane) and MWCNT (multi-walled carbon nanotubes), is examined and contrasted with a simulated model of the same active layer. The simulated model tactile sensor is subjected to a range of pressure loads, ranging from 1N to 11N.

The load block delivers these loads with a steady incremental step size measuring 2N in the normal direction. The variation in resistance resulting from the application of external pressure is compared to the instantaneous response of the sensor [11], as seen in Figure 7.

When comparing the output response of both sensors, it is important to consider the difference in physical dimensions. The real-time tactile sensor has a size of 1mm x1 mm, while the simulated model is 10mm x 10mm in size. Additionally, the real-time model uses electrodes, which is not the case in the simulated model.

Another significant distinction is that the real-time nano conduction mechanism operates according to the tunnelling effect, while the simulation is based on piezoresistive principles. The simulated response closely mimicked the real-time sensor response up to a pressure of 6N. Furthermore, the simulated pressure sensor response showed the same trajectory consistently as the real-time model, albeit at a higher magnitude. In general, there is a strong correlation between the behavior of real-time and simulated sensors.

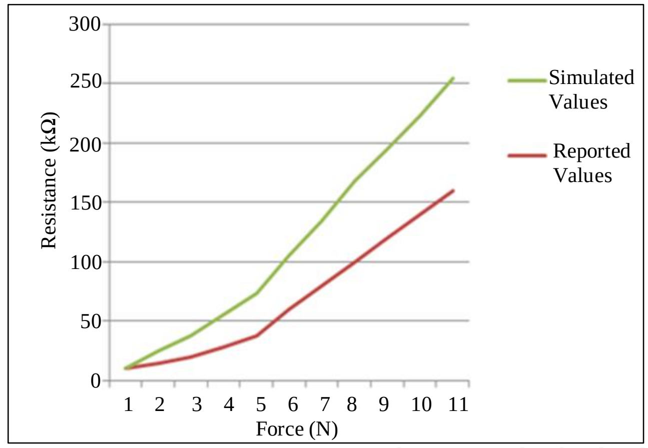

Fig. 7 Piezo resistive response comparison between simulated and real time E-skin tactile sensor with MWCNT+PDMS sensing material

5. Conclusion

The modelling of piezoresistive tactile sensors yielded useful insights into the electrical and mechanical characteristics of the piezoresistive-based pressure sensor when subjected to various loads and materials on its active layer. SBS + MWCNT is a highly conformable active layer. However, the PDMS + MWCNT-based sensory layer has a more linear range of transduction and, hence more suitable for humanoid robot E-skin applications.

Our simulation model-based research minimized the chances of material wastage and also saved time by performing repeated examinations of various materials on a single standardized template. Simulated design has a pivotal role in the optimization of the overall design layout. It helps engineers predict the space needed for various components on the E-skin in the field of large-area electronics.

In addition, the study revealed firsthand information on issues that may crop up in the screen-printing process in real time. The mechanical behavior simulation aids in creating a blueprint of the sensor layout design when a grid of sensors is positioned on the substrate. By examining the influence of contact resistance on the sensor output, one may notice more compelling findings in terms of the electrical reaction when electrodes are positioned in the future.

References

[1] Stefan C.B. Mannsfeld et al., “Highly Sensitive Flexible Pressure Sensors with Microstructured Rubber Dielectric Layers,” *Nature Materials*, vol. 9, pp. 859-864, 2010. [CrossRef] [Google Scholar] [Publisher Link]

[2] K. Yamada et al., “A Sensor Skin Using Wire-Free Tactile Sensing Elements Based on Optical Connection,” *Proceedings of the 41st SICE Annual Conference*, Osaka, Japan, vol. 1, pp. 131-134, 2002. [CrossRef] [Google Scholar] [Publisher Link]

[3] Haoxuan He et al., “A Flexible Self-Powered T-ZnO/PVDF/Fabric Electronic-Skin with Multi-Functions of Tactile-Perception, Atmosphere-Detection and Self-Clean,” *Nano Energy*, vol. 31, pp. 37-48, 2017. [CrossRef] [Google Scholar] [Publisher Link]
[4] Stefano Stassi et al., “Flexible Tactile Sensing Based on Piezoresistive Composites: A Review,” *Sensors*, vol. 14, no. 3, pp. 5296-5332, 2014. [CrossRef] [Google Scholar] [Publisher Link]
[5] Moinuddin Ahmed et al., “MEMS Force Sensor in a Flexible Substrate Using Nichrome Piezoresistors,” *IEEE Sensors Journal*, vol. 13, no. 10, pp. 4081-4089, 2013. [CrossRef] [Google Scholar] [Publisher Link]
[6] Lin Li et al., “Flexible Pressure Sensors for Biomedical Applications: From Ex Vivo to In Vivo,” *Advanced Materials Interfaces*, vol. 7, no. 17, 2020. [CrossRef] [Google Scholar] [Publisher Link]
[7] Harish Devaraj et al., “The Development of Highly Flexible Stretch Sensors for a Robotic Hand,” *Robotics*, vol. 7, no. 3, pp. 1-13, 2018. [CrossRef] [Google Scholar] [Publisher Link]
[8] Luxian Wang et al., “PDMS/MWCNT-Based Tactile Sensor Array with Coplanar Electrodes for Crosstalk Suppression,” *Microsystems & Nanoengineering*, vol. 2, pp. 1-8, 2016. [CrossRef] [Google Scholar] [Publisher Link]
[9] Miao Lu, Amine Bermak, and Yi-Kuen Lee, “Fabrication Technology of Piezoresistive Conductive PDMS for Micro Fingerprint Sensors,” *2007 IEEE 20th International Conference on Micro Electro Mechanical Systems (MEMS)*, Hyogo, Japan, pp. 251-254, 2007. [CrossRef] [Google Scholar] [Publisher Link]
[10] Min-Young Cho et al., “A Styrene-Butadiene Rubber (SBR)/Carbon Nanotube-Based Smart Force Sensor for Automotive Tire Deformation Monitoring,” *Proceedings of Nanosensors, Biosensors, and Info-Tech Sensors and Systems*, vol. 9802, 2016. [CrossRef] [Google Scholar] [Publisher Link]
[11] P. Costa et al., “Effect of Carbon Nanotube Type and Functionalization on the Electrical, Thermal, Mechanical and Electromechanical Properties of Carbon Nanotube/Styrene-Butadiene-Styrene Composites for Large Strain Sensor Applications,” *Composites Part B: Engineering*, vol. 61, pp. 136-146, 2014. [CrossRef] [Google Scholar] [Publisher Link]
[12] Saleem Khan et al., “Conformable Tactile Sensing Using Screen Printed P (VDF-TrFE) and MWCNT-PDMS Composites,” *IEEE-Sensors*, Valencia, Spain, pp. 862-865, 2014. [CrossRef] [Google Scholar] [Publisher Link]
[13] Bokeon Kwak, and Joonbum Bae, “Integrated Design and Fabrication of a Conductive PDMS Sensor and Polypyrrole Actuator Composite,” *IEEE Robotics and Automation Letters*, vol. 5, no. 3, pp. 3753-3760, 2020. [CrossRef] [Google Scholar] [Publisher Link]
[14] S. Anand Selvin et al., “Design and Simulation of Carbon Nanotube based Piezoresistive Pressure Sensor,” *Proceedings of the 2011 COMSOL Conference*, Bangalore, pp. 1-5, 2011. [Google Scholar]
[15] Intelligent Materials Private Limited, Nanoshel MWCNT Specification Certificate, 2023. [Online]. Available: https://www.nanoshel.in/awards-and-memberships.html
[16] M. Tintelott et al., “Sensitivity of Flexible Pressure Sensors Mounted on Curved Surfaces,” *Sensors and Measuring Systems; 19th ITG/GMA-Symposium*, Nuremberg, Germany, pp. 1-4, 2018. [Google Scholar] [Publisher Link]
[17] Smooth-On, ECOFLEX_00-30 Datasheet. [Online]. Available: https://www.smooth-on.com/products/ecoflex-00-30/
[18] Morteza Amjadi, Yong Jin Yoon, and Inkyu Park, “Ultra-Stretchable and Skin-Mountable Strain Sensors Using Carbon Nanotubes-Ecoflex Nanocomposites,” *Nanotechnology*, vol. 26, no. 37, 2015. [CrossRef] [Google Scholar] [Publisher Link]